International Journal of Heat and Mass Transfer 138 (2019) 1142–1153

Contents lists available at ScienceDirect

International Journal of Heat and Mass Transfer

journal homepage: www.elsevier.com/locate/ijhmt

A revised performance evaluation method for energy saving effectiveness of heat transfer enhancement techniques

Wen-Tao Ji *, Ju-Fang Fan, Chuang-Yao Zhao, Wen-Quan Tao

Key Laboratory of Thermo-Fluid Science and Engineering of MOE, School of Energy and Power Engineering, Xi'an Jiaotong University, Xi'an 710049, China

ARTICLE INFO

Article history:
Received 21 August 2018
Received in revised form 13 April 2019
Accepted 26 April 2019

Keywords:
Heat transfer enhancement
Heat exchangers
Performance evaluation

ABSTRACT

In this paper, a revised performance evaluation method was proposed to estimate the thermal hydraulic performance of various heat transfer enhancement techniques. The energy saving effectiveness for the enhanced structures can be identified via a plot. In the plot, Reynolds number and the efficiency index $\ln(Nu_e/Nu_r)/\ln(f_e/f_r)$ are taken as the X and Y coordinates, respectively. The efficiency can be ranked into four different levels. For experimental data or simulation results in Level 1, enhanced heat transfer is accompanied with more power consumption. The data in Level 2 is that the heat transfer can be intensified at the same pumping power. In Level 3, it is characterized by the augmented heat transfer at the same pressure drop. The efficiency in Level 4 is the highest. The ratio of heat transfer augmentation is higher than the increment ratio of friction factor at the same Reynolds number. Four levels correspond to four horizontal regions with Level 1 at the bottom and Level 4 at the top. The data at higher levels in the ordinate will be more competitive for energy saving. The examples on how to use the method for evaluating the performance of enhanced surfaces and typical heat exchangers were also presented.

1. Introduction

In order to reduce the energy and material consumption, a lot of efforts have been made to enhance the heat transfer. The passive heat transfer enhancement techniques include roughed surface, extended surface, swirl generators, etc. It is a common knowledge that any enhancement technique which affects the heat transfer will also inevitably affect the friction factor or pumping power as well. This fact is caused by the increased skin friction in redeveloping the boundary layer and the occurrence of recirculation flow around the enhanced structures. If the height or number of fins per circle is increased for a single phase internal pipe flow, it would lead to an increased pressure drop. Normally, prediction of heat transfer coefficient is related with friction factor [1–3]. If one only simply calculated the heat transfer enhancement ratio, an unfair comparison may result in. Thus, it will inevitably involve the performance evaluation which can take into account the full merits of friction and heat transfer. Through the efficiency evaluation methods, the parameters which yield the best performance can be selected.

There are a lot of factors when evaluating the effectiveness of an enhanced surface. It includes the reliability, efficiency, economic cost, operating cost, and maintenance cost. It is impossible to take all these factors into account. Therefore, a clear and simple definition, user friendly statement, easy to understand and use are rather important.

To date, different approaches have been proposed for the performance assessment. The constraints involve higher heat transfer performance, equal pressure drop, same flow rate and pumping power. Generally, the evaluating methods include the following categories. One is on the basis of the first-law thermodynamics. It defines the performance benefits of a heat transfer unit with enhanced surfaces, relative to that of reference surface. The other methods are mostly derived on the basis of the second law of the thermodynamics [4]. Entropy production should be determined with this method. It is meaningful from the academic point of view. However, it was a little bit more mathematically complex than the first method. At least so far the first category seems to be more widely used in the engineering applications according to the literature survey.

For the first evaluating method, the criteria is typically under the constraints of same flow rate, equal pump power, constant surface area, or equal pressure drop [5,6]. Webb [5] classified the three typical design objective as reduced material consumption, reduced pumping power and increased heat transfer efficiency. For design objective of increasing the heat transfer at the same flow rate, equal pump power or fix geometry, some typical efficiency indexes based on the first law of thermal dynamics include:

* Corresponding author.
E-mail address: wentaoji@xjtu.edu.cn (W.-T. Ji).

https://doi.org/10.1016/j.ijheatmasstransfer.2019.04.128
0017-9310/

Nomenclature

A	heat transfer surface area, m^2
c_1, c_2	coefficients in Eqs. (1) and (2)
$C_{Q,i}$	the ratio of Nusselt number between enhanced and reference surfaces under different constraints
D	hydraulic diameter, m
f	friction factor
j	j-factor, Colburn factor
k	heat transfer coefficient, $W/(m^2 K)$
k_i	index in Eq. (26)
L	length of the flow passage, m
m_1, m_2	indices in Eqs. (1) and (2)
Nu	Nusselt number
P	pumping power, W
Q	heat transfer rate, W
Re	Reynolds number
V	flow velocity of fluid, m/s
Δp	pressure drop, Pa
Δt	wall-to-fluid temperature difference, K
η	efficiency index in literature
λ	thermal conductivity of fluid, W/(m K)
ρ	fluid density, kg/m^3

Subscripts

r	reference surface (heat exchanger)
e	enhanced surface
m	mean value
P	under equal pumping power
Re	under equal Reynolds number
V	under equal flow rate
Δp	under equal pressure drop

$$\eta_1 = \frac{Nu/Nu_r}{f/f_r}, \quad \eta_2 = \frac{St/St_r}{(f/f_r)^{1/3}}, \quad \eta_3 = \frac{Nu/Nu_r}{(f/f_r)^{1/3}}$$

In the above equations, the parameters *f, Nu* and *St* represent friction factor, Nusselt number and Stanton number, respectively. Subscript "r" refers to the surface for comparison. Without the subscript refers to the enhanced surface.

In many instances, heat transfer rate need to be evaluated with specified flow rate and reduction of flow rate is not permitted. It belongs to the category of fixed geometry criteria (FG-1) of Webb [5] for fixed entering fluid temperatures. The index, η_2 and η_3 are usually used to identify the performance of augmented surface at equal pump power. It belongs to the category of fixed geometry criteria (FG-2) of Webb [5] for fixed entering fluid temperatures η_2 was proposed by Webb and Eckert [7]. The objective of fixed flow area (FV-1) is also usually used under the constraint of equal pressure drop. This criterion maintains the constant flow cross section area. The heat transfer area could be reduced via reduced tubing length for constant pressure drop.

Fan et al. [8] proposed a plot to assess the efficiency of different heat transfer augmentation surfaces. The assessment was geometrically related to the selected referenced surface. The heat transfer of augmented and that of reference surface can be evaluated with the plot. In their plot, $\ln(Nu_e/Nu_r)$ and $\ln(f_e/f_r)$ were taken as the X and Y coordinates, respectively. Subscript "e" refers to the enhanced surface. Experimental test data or simulation results of any enhancement technique can be showed in the figure and the level of efficiency can also be clearly demonstrated. However, a weakness of the plot is that Reynolds number is not explicitly expressed. The changes of heat transfer with Reynolds number cannot be shown explicitly in the plot. The data for laminar flow and turbulent flow might occur in the same positions. It might lead to confusion. According to the analysis on the currently available performance evaluation methods and based on the evaluation plot proposed by Fan et al. [8], another performance evaluation method is proposed in this paper.

In Section 2, the equations for the evaluation method would firstly be introduced. In Section 3, the examples on how to use the method for the enhanced tubes and typical heat exchangers will be illustrated. Section 4 is the conclusion.

2. Derivation of formulas for the revised performance evaluation method

Normally, the performance evaluation criteria can be divided into two basic categories. One is that considering all the influencing factors including the fluid properties. It is also named as a "general methods". For detailed comparisons between heat transfer surfaces, the general methods can be used as indicators in the first instance. When using this method, it involves performing a complete heat exchanger or heat transfer analysis. It is particularly difficult to arrive at a general conclusion that is valid for varying fluid properties. The other method is based on some limited assumptions, e.g. constant thermo-physical properties of fluid. For simplicity, the fluid properties are assumed to be the same for both the reference and enhanced surfaces. If the inlet temperature is the same, the difference for the thermo physical properties is normally not large. The error due to these assumptions is small for heat exchangers operating with low temperature differences. The second method was more widely used in the performance evaluations [5,7].

The revised performance evaluation method is generally on the basis of the assumptions presented by Fan et al. [8], which is also same as the assumptions made for the Fixed Geometry (FG) criteria of Webb et al. [5,7], with the objective of intensifying heat transfer without changing the size of nominal heat transfer and flow area. The surface area can be based on either the actual or nominal surface area. The actual area can be used for the finned surfaces (including the extra area provided by the fins), but the actual area of different structures for enhancement techniques is normally difficult to measure. If the enhanced structure is randomly distributed, it is even impossible to obtain the actual surface area. The nominal area is based on the original area of the unfinned surface. This is a simplified approach. All of the surfaces are compared to plain surfaces having no enhancements. The area of the plain surface is the nominal area. If we would like to compare the heat transfer performance based on the same root surface, nominal area will be more desirable.

These performance evaluation methods consider the comparison of heat transfer performance with constraints of constant nominal area, flow rates, pumping power and hydraulic losses. The reference surface can be a plain surface or a typical enhanced surface. As the flow rate for identical pumping power and pressure drop is usually different to enhanced and referenced surfaces, the thermal hydraulic performance is normally evaluated at the same Reynolds number. The fluid inlet temperature should also be the same.

The present evaluation method is on the basis of the following assumptions for the augmented and reference surface:

(1) Constant fluid thermophysical properties, e.g. Prandtl number, viscosity [5].
(2) Nominal heat transfer area is the same.

(3) Nominal flow area and basic geometry are the same, e.g. $D_e/D_r = 1$.
(4) Dimensionless characteristic number is the same, e.g. *Re*.

The method is primarily used for the one-for-one comparison of reference and enhanced surfaces (heat exchangers). For the frequently used fluids, the assumptions can be easily satisfied.

The derivations of some basic equations for the evaluation method are also similar as Fan et al. [8]. For the reader's convenience, it is briefly described as follows. Normally, friction factor and Nusselt number of reference surface or heat exchanger can be obtained or correlated.

$$f_r(Re) = c_1 Re^{m_1} \tag{1}$$

$$Nu_r(Re) = c_2 Re^{m_2} \tag{2}$$

The reference surface can also be an augmented surface. For the single-phase pipe flow, using the Blasius equation, ($f = 0.046Re^{-0.25}$) and Dittus-Boelter equation ($Nu = 0.023Re^{0.8}Pr^n$). As the thermophysical properties of fluid for enhanced and reference structure are the same, *f* and *Nu* of reference plain pipe could be: $f_r(Re) = c_1 Re^{-0.25}$ and $Nu_r(Re) = c_2 Re^{0.8}$.

At the same Reynolds number, the ratio of Nusselt number and friction factor for augmented and referenced surfaces are defined as follows:

$$\left(\frac{f_e}{f_r}\right)_{Re} = \frac{f_e(Re)}{f_r(Re)} \tag{3}$$

$$\left(\frac{Nu_e}{Nu_r}\right)_{Re} = \frac{Nu_e(Re)}{Nu_r(Re)} \tag{4}$$

In the above equation, the subscript "*Re*" means that the ratio of *Nu* or *f* is obtained at the same Reynolds number.

There are normally three constraints for the performance evaluation methods. They are at the same pressure drop, flow rate and pump power. If the pump power or pressure drop is kept constant, Reynolds number for the augmented and reference surfaces should be different. Hence, for the comparison of performance at the same pump power and pressure drop, the corresponding Reynolds number should be different. The comparison at the same flow rate can use Eqs. (3) and (4).

For different Reynolds number, the ratios of *Nu* and *f* for augmented surface and reference one can be expressed as:

$$\left(\frac{f_e}{f_r}\right)_{\text{at different } Re} = \frac{f_e(Re)}{f_r(Re_r)} \tag{5}$$

$$\left(\frac{Nu_e}{Nu_r}\right)_{\text{at different } Re} = \frac{Nu_e(Re)}{Nu_r(Re_r)} \tag{6}$$

Substituting Eqs. (1) into (3), friction factor for the augmented surface at any Reynolds number is:

$$f_e(Re) = \left(\frac{f_e}{f_r}\right)_{Re} \cdot c_1 Re^{m_1} \tag{7}$$

Substituting Eqs. (1) into (5) for $f_r(Re_r)$ and Eqs. (7) into (5) for $f_e(Re)$, the expression for the ratio of friction factor at any different *Re* can be written as:

$$\left(\frac{f_e}{f_r}\right)_{\text{at different } Re} = \frac{f_e(Re)}{f_r(Re_r)} = \left(\frac{f_e}{f_r}\right)_{Re}\left(\frac{Re}{Re_r}\right)^{m_1} \tag{8}$$

Substituting Eqs. (2) into (4) for $Nu_r(Re)$, *Nu* for the augmented surface at different *Re* is:

$$Nu_e(Re) = \left(\frac{Nu_e}{Nu_r}\right)_{Re} \cdot c_2 Re^{m_2} \tag{9}$$

Substituting Eqs. (2) into (6) for $Nu_r(Re_r)$ and Eqs. (9) into (6) for $Nu_e(Re)$, the *Nu* ratios at any different *Re* could be:

$$\left(\frac{Nu_e}{Nu_r}\right)_{\text{at different } Re} = \frac{Nu_e(Re)}{Nu_r(Re_r)} = \left(\frac{Nu_e}{Nu_r}\right)_{Re}\left(\frac{Re}{Re_r}\right)^{m_2} \tag{10}$$

The two equations above indicated that if the ratios of *f* and *Nu* for the augmented and reference surfaces at the same *Re* are obtained, then the ratios of *Nu* and *f* at any different *Re* can also be determined.

The objective of most evaluation methods focuses on the increment ratio of the heat transfer. There are conventionally three restraints for this ratio. The heat transfer rate, pressure drop and pump power can be defined as [9]:

$$Q = kA\Delta T; \quad \Delta p = 2f\frac{L}{D}\frac{V^2}{\rho}; \quad P = A \cdot V\Delta p$$

The ratio of pump power for augmented and reference surfaces is:

$$\frac{P_e}{P_r} = \frac{(A_c \cdot V \cdot \Delta p)_e}{(A_c \cdot V \cdot \Delta p)_r} = \frac{(A_c \cdot V \cdot f \cdot L \cdot \rho \cdot V^2/D)_e}{(A_c \cdot V \cdot f \cdot L \cdot \rho \cdot V^2/D)_r} \tag{11}$$

According to the four assumptions, we can write:

$$\frac{(A_c \cdot L \cdot \rho \cdot /D)_e}{(A_c \cdot L \cdot \rho \cdot /D)_r} = 1 \tag{12}$$

Combine the Eqs. (12) and (11), the ratio of pumping power is as follows:

$$\frac{P_e}{P_r} = \frac{(f \cdot V^3)_e}{(f \cdot V^3)_r} = \frac{f_e \cdot Re^3}{f_r \cdot Re_r^3} = \frac{f_e(Re)}{f_r(Re_r)}\left(\frac{Re}{Re_r}\right)^3 \tag{13}$$

According to Eq. (13), at the same pumping power, the ratio of friction factor for augmented and reference surfaces at various *Re* is:

$$\left(\frac{f_e}{f_r}\right)_{at\ \text{different } Re} = \frac{f_e(Re)}{f_r(Re_r)} = \left(\frac{Re}{Re_r}\right)^{-3} \tag{14}$$

Combine the Eqs. (14) and (8), the ratio of *Re* at the same pumping power is:

$$\frac{Re}{Re_r} = \left(\frac{f_e}{f_r}\right)_{Re}^{\frac{-1}{3+m_1}} \tag{15}$$

Moreover, substituting Eqs. (14) into (8), the ratio of *Nu* at same pumping power is:

$$\left(\frac{Nu_e}{Nu_r}\right)_{\text{at same pumping power}} = \frac{Nu_e(Re)}{Nu_r(Re_r)} = \left(\frac{Nu_e}{Nu_r}\right)_{Re}\left(\frac{Re}{Re_r}\right)^{m_2} = \left(\frac{Nu_e}{Nu_r}\right)_{Re}\left(\frac{f_e}{f_r}\right)_{Re}^{\frac{-m_2}{3+m_1}} \tag{16}$$

Eq. (16) yield:

$$\left(\frac{Nu_e}{Nu_r}\right)_{\text{at the same pumping power}} = \left(\frac{Nu_e}{Nu_r}\right)_{Re} \Big/ \left(\frac{f_e}{f_r}\right)_{Re}^{\frac{m_2}{3+m_1}} \tag{17}$$

Eq. (17) shows the ratio of *Nu* for augmented and reference surfaces at the same pumping power. The Reynolds number is usually different for the augmented and reference surfaces at the identical pumping power consumption. At the same pumping power, Eq. (17) can demonstrate whether the enhanced surface can really intensify the heat transfer.

At the constraint of same pressure drop, we can obtain a similar equation.

$$\frac{\Delta p_e}{\Delta p_r}=\frac{(f\cdot L\cdot \rho\cdot V^2/D)_e}{(f\cdot L\cdot \rho\cdot V^2/D)_r} \tag{18}$$

Based on the four assumptions:

$$\frac{(A_c\cdot L\cdot \rho\cdot /D)_e}{(A_c\cdot L\cdot \rho\cdot /D)_r}=1 \tag{19}$$

Eqs. (18) and (19) give:

$$\frac{\Delta p_e}{\Delta p_r}=\frac{(f\cdot V^2)_e}{(f\cdot V^2)_r}=\frac{f_e(Re)}{f_r(Re_r)}\left(\frac{Re}{Re_r}\right)^2 \tag{20}$$

According to (20), at the constraint of same pressure drop, ratio of friction factor for augmented surface over reference one is calculated by the equation:

$$\frac{f_e}{f_r}=\frac{f_e(Re)}{f_r(Re_r)}=\left(\frac{Re}{Re_r}\right)^{-2} \tag{21}$$

Combine the Eq. (21) and (8), the ratio of *Re* at the same pressure drop is:

$$\frac{Re}{Re_r}=\left(\frac{f_e}{f_r}\right)_{Re}^{\frac{-1}{2+m_1}} \tag{22}$$

Moreover, substituting Eqs. (22) into (10), ratio of *Nu* at the same pressure drop is:

$$\begin{aligned}\left(\frac{Nu_e}{Nu_r}\right)_{\text{at same pressure drop}}&=\frac{Nu_e(Re)}{Nu_r(Re_r)}=\left(\frac{Nu_e}{Nu_r}\right)_{Re}\left(\frac{Re}{Re_r}\right)^{m_2}\\&=\left(\frac{Nu_e}{Nu_r}\right)_{Re}\left(\frac{f_e}{f_r}\right)_{Re}^{\frac{-m_2}{2+m_1}}\end{aligned} \tag{23}$$

Eq. (23) gives:

$$\left(\frac{Nu_e}{Nu_r}\right)_{\text{at same pressure drop}}=\left(\frac{Nu_e}{Nu_r}\right)_{Re}/\left(\frac{f_e}{f_r}\right)_{Re}^{\frac{m_2}{2+m_1}} \tag{24}$$

Eq. (24) shows the ratio of *Nu* at the constraint of same pressure drop. Whether the enhanced surface can really enhance the heat transfer depend on if this ratio is more than 1.

For the constraint of same flow rate:

$$\frac{Nu_e}{Nu_r}=\left(\frac{Nu_e}{Nu_r}\right)_{Re} \tag{25}$$

Increment of heat transfer is often compared with increment of friction factor at the same flow rate [10–12]. This is a higher level of energy efficiency more difficult to obtain compared with the equal pump power and pressure drop.

Normally, *Nu* and *f* at the same *Re* for the enhanced and reference surface can be obtained in the experiment. The performance of the heat transfer enhancement techniques could be evaluated with these experimental data. According to the above analysis, the levels of efficiency can be based on the ratio of *Nu* and *f* at equal *Re*. It should be noted that Reynolds number for *Nu* and *f* are mostly not exactly match in experiment. In these cases, *Nu* and *f* for reference surface can be fitted to polynomial function to suit the requirements for equal Reynolds number. Based on the analysis above, we can transform the Eqs. (17), (24) and (25) into the following general form from the three typical constraints.

$$C_{Q,i}=\left(\frac{Nu_e}{Nu_r}\right)_{Re}\Big/\left(\frac{f_e}{f_r}\right)_{Re}^{k_i}\quad(i=P,\Delta p,V) \tag{26}$$

where $P, \Delta p,$ *and* V represent the constraints of equal pump power, pressure drop and flow rate. Compare Eqs. (26) and (17), (24) and (25) give:

$$k_P=\frac{m_2}{3+m_1},\quad k_{\Delta p}=\frac{m_2}{2+m_1},\quad k_V=1.0 \tag{27}$$

For a convection heat transfer problem, the variable m_1 and m_2 were normally in the range of $-1\le m_1<0$ and $0<m_2<1$. Therefore, the value of k_i can be obtained as

$$0<\frac{m_2}{3+m_1}<\frac{m_2}{2+m_1}<1 \tag{28}$$

To augment the heat transfer at the identical pressure drop, it requires that

$$\left(\frac{Nu_e}{Nu_r}\right)_{Re}/\left(\frac{f_e}{f_r}\right)_{Re}^{k_{\Delta p}}\geqslant 1 \tag{29}$$

When it equals 1, it means that the heat transfer enhancement ratio Nu_e/Nu_0 equals to 1. That is

$$\left(\frac{f_e}{f_r}\right)_{Re}^{k_{\Delta p}}=\left(\frac{Nu_e}{Nu_r}\right)_{Re} \tag{30}$$

By taking the logarithm of Eq. (29), it is

$$\ln\left(\frac{Nu_e}{Nu_r}\right)_{Re}\Big/\ln\left(\frac{f_e}{f_r}\right)_{Re}\geqslant k_{\Delta p} \tag{31}$$

For the level standard of heat transfer enhancement at same pumping power, it requires that:

$$\ln\left(\frac{Nu_e}{Nu_r}\right)_{Re}\Big/\ln\left(\frac{f_e}{f_r}\right)_{Re}\geqslant k_P \tag{32}$$

The level standard of heat transfer intensification at same flow rate requires that:

$$\ln\left(\frac{Nu_e}{Nu_r}\right)_{Re}\Big/\ln\left(\frac{f_e}{f_r}\right)_{Re}\geqslant k_V \tag{33}$$

Eq. (26) is known as the function of Reynolds number. If we take *Re* as the abscissa and $k_i=\ln\left(\frac{Nu_e}{Nu_r}\right)_{Re}/\ln\left(\frac{f_e}{f_r}\right)_{Re}$ as the ordinate, k_i is the criterion and index to characterize the energy saving efficiency of a specific heat transfer augmentation technique. The effectiveness of a heat transfer augmentation technique can be shown in a plot, where k_i is the ratio of $\ln(Nu_e/Nu_r)$ over $\ln(f_e/f_r)$ at the same Reynolds number. The boundary line of the efficiency of the augmented heat transfer surfaces is k_P, $k_{\Delta p}$ and k_V. If $\ln\left(\frac{Nu_e}{Nu_r}\right)/\ln\left(\frac{f_e}{f_r}\right)$ is higher than $k_{\Delta p}$, it means that the heat transfer could be intensified at the same pressure drop. Equal pump power or flow rate are similar. Heat transfer performance of an enhanced surface or heat exchanger under various constraints can be assessed with this ratio. The levels of efficiency for heat transfer augmentation techniques can be indicated by this index, k_i. According to the above equations, an efficiency assessment plot for the heat transfer augmentation techniques is presented in Fig. 1. It is a log-log plot.

Come here it is interested to discuss the difference of the present analysis and that made in Fan et al. [8]. The differences are three-fold. The major difference is that in [8] the heat transfer enhanced ratio of the augmented surface over the referenced one is taken as the criterion, while the ratio of Nusselt number is the criterion in this paper. Second, in [8] it has an assumption that the temperature difference between the heat transfer wall and fluid is same for the enhanced and referenced structures, which is not very reasonable for practical situation. In this method we do not make such an assumption. Third difference is that from Eq. (26) the ratio of $\ln\left(\frac{Nu_e}{Nu_r}\right)/\ln\left(\frac{f_e}{f_r}\right)$ at the same Reynolds number is taken as the comprehensive thermos-hydraulic criterion for evaluating the performance of an enhanced structure and ln*Re* as the abscissa of the plot which make the effect of Reynolds number being explicitly reflected.

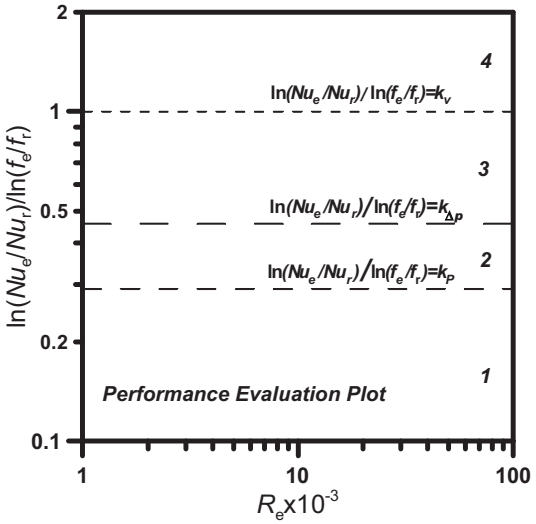

Fig. 1. The performance evaluation plot.

For the reference surface, the experimental or simulation data for friction factor and Nusselt number can mostly be fitted into the following exponential relationship:

$$f_r(Re) = c_1 Re^{m_1}$$

$$Nu_r(Re) = c_2 Re^{m_2}$$

For the turbulent pipe flow, if the plain tube is regarded as the reference surface. Using the Blasius equation, ($f = 0.046Re^{-0.25}$) and Dittus-Boelter equation ($Nu = 0.023Re^{0.8}Pr^n$), $m_1 = -0.25$, $m_2 = 0.8$.

$$k_P = \frac{m_2}{3+m_1} = 0.290, \quad k_{\Delta p} = \frac{m_2}{2+m_1} = 0.457, \quad k_V = 1.0$$

These three values can divide the coordinates into four parts. Normally, the magnitude of the indexes is $k_P < k_{\Delta p} < k_V$. The experimental measurements located at higher levels in the plot have the higher performance efficiency. k_P, $k_{\Delta p}$ and k_V are the boundaries of different efficiency level standards.

Normally, we select the plain or typical enhanced surface as the reference surface. The augmented surface should have higher pressure drop and friction factor than the referenced one. The f_e/f_r and Nu_e/Nu_r are higher than 1. Hence, $\ln(f_e/f_r)$ and $\ln(Nu_e/Nu_r)$ should be larger than 0. If f_e/f_r and Nu_e/Nu_r are less than 1, we may use the Log-Modulus transformation for the comparison.

As shown in Fig. 1, the performance evaluation plot can be divided into four typical levels of energy efficiency indicated by the numbers 1, 2, 3, and 4. The data in Level 1 standard is characterized by enhanced heat transfer while contribute to more power consumption. It doesn't save energy in this region. The data in Level 2 indicates that the heat transfer can be intensified at the same pumping power. In other words, the enhanced surface has a higher heat transfer coefficient than the reference one at the identical pump power. If the Nusselt number for the augmented surface is larger, the heat transfer rate for the augmented surface is higher. In Level 3, the heat transfer could be enhanced at the same pressure drop. In other words, the augmented surface has a higher heat transfer coefficient than the reference one at the same pressure drop. The data of any heat transfer enhancement technique in Level 4 is the most beneficial. In this region, the ratio of heat transfer coefficient is higher than the ratio of friction factor at the same Reynolds number. That is more constrictive and most difficult to obtain. The experimental data that located in higher levels in the coordinate will be more effective in energy saving.

For the data in the boundary line between Level 1 and 2, P_e/P_r equals 1. It indicates that at the same Reynolds number, the heat transfer is enhanced and the augmented and reference surfaces have the same pumping power. To enhance heat transfer at the same pump power, the lowest requirement is that $(Nu_e/Nu_r)_{\text{at same pumping power}} > 1$. For the data in the border of Level 2 and 3, it is under the condition of $(Nu_e/Nu_r)_{Re} > 1$ and $\Delta p_e/\Delta p_r = 1$.

To obtain an increased heat duty for the fixed geometry, at the different constraints, the higher value of Nu_e/Nu_r, the better of the enhancement technique. This plot can be used to showing the energy-saving effectiveness and identify whether the heat transfer intensification methods could really save energy.

Normally, the reference surface has a lower friction factor and Nusselt number. To assess the heat transfer performance of internal single-phase pipe flow, plain tube are usually used as the reference surface. For the different types of fins to enhance the air-side heat transfer, the plain fin is mostly used as the reference surface. In the evaluation plot, there are two cases that the data will fall outside of the coordinate. The first case is heat transfer is not intensified but pressure drop increases. It has no practical value and will not be used in reality. The other case is that the heat transfer increases while friction factor is reduced. It is also quite uncommon in practice. Therefore, these cases will not be discussed in this paper.

3. Examples of using the performance evaluation method

The evaluation method can be used to identify the energy-saving effectiveness of different heat transfer augmentation techniques. It can also indicate which regime the heat transfer enhancement technique are the most optimal, in the laminar, transition, or turbulent flow. The performance evaluation method described above can be simplified into the following steps:

(1) Select the plain or appropriate enhanced surface (or heat exchanger) as the reference.
(2) Define or obtain the correlations for Nu and f for the reference surface (or heat exchanger) as a function of Re. Normally, the correlation can be fitted in the form of $f_r = c_1 Re^{m_1}$ and $Nu_r = c_2 Re^{m_2}$.
(3) Determine $k_i = \ln\left(\frac{Nu_e}{Nu_r}\right)/\ln\left(\frac{f_e}{f_r}\right)$ at the same Re.
(4) Determine the levels of efficiency, k_P, $k_{\Delta p}$ and k_V in the coordinates ($k_P = \frac{m_2}{3+m_1}$; $k_{\Delta p} = \frac{m_2}{2+m_1}$; $k_V = 1.0$).
(5) Show k_i of experimental data versus Re, k_P, $k_{\Delta p}$and k_V in the plot.

If we can only obtain the ratios of $\frac{Nu_e}{Nu_0}$and $\frac{f_e}{f_r}$ for the reference and enhanced surfaces at the same Reynolds number, or the correlation cannot be fitted with the forms of $f_r = c_1 Re^{m_1}$ and $Nu_r = c_2 Re^{m_2}$, the evaluation method can also be used. However, k_P, $k_{\Delta p}$ and k_V cannot be determined in these circumstances. Following are some examples using this performance evaluation method.

3.1. Internal pipe flow

Different types of heat transfer enhancement techniques were used for the single-phase pipe flow [13–15]. For internal pipe flow, the enhancement techniques involve the fins, corrugations, dimples and tape inserts or wires (see Fig. 2). Compound heat transfer enhancement techniques might also be used. Tables 1–4 listed some typical experimental studies of heat transfer augmentation techniques for internal pipe flow.

The assessment is on the basis of reference plain tube. The correlations to determine f of plain pipe is Blasius correlation,

($f = 0.046Re^{-0.25}$) and Dittus-Boelter equation ($Nu = 0.023Re^{0.8}Pr^{n}$). The efficiency indexes are: $m_1 = -0.25$, $m_2 = 0.8$. The other parameters are: $k_P = \frac{m_2}{3+m_1} = 0.290$, $k_{\Delta p} = \frac{m_2}{2+m_1} = 0.457$, and $k_V = 1.0$.

Tables 1–4 show the survey on the experimental data for internal fins, tape inserts, corrugations, dimples and different types of roughness, respectively. Figs. 3–6 show the performance evaluation plots for four typical heat transfer augmentation techniques. As shown in the figures, the efficiency index for internally finned tubes is mostly higher than other three heat transfer enhancement techniques. Most of the experimental data were in Level 4 or that near Level 4. The friction factor of air for low and high fin is normally higher compared with micro fins. Hence, three tubes with low-fin and high-fin have the lowest efficiency indexes in the plot (Fig. 3). It also indicates that the increment of heat transfer for water is the largest at different Reynolds number.

The revised performance assessment plot has the same predication result as the plot in [8,14,15]. The tube in Jensen and Vlakancic [29], still had higher efficiency in the present plot. The experimental data in Wang et al. [10], also located in different regions in the plot. However, the present plot can clearly identify the thermo-hydraulic efficiency of the tubes at different Reynolds number.

For the internal inserts (Fig. 4), as increase of *Re*, the efficiency is decreasing for most of studies. It indicated the twisted tape inserts is suitable for that at lower Reynolds number. Some of the experimental data was in the region of Level 1. This is the region that despite the heat transfer is enhanced to some extent, while it doesn't save energy. The data in this region is mostly the compound heat transfer enhancement techniques. Apart from the data located in Level 1, a lot of data were in Level 2. Tubes located in Level 3 is the most efficient tape parameters, such as the tube in Smithberg and Landis [22].

For the corrugated tubes, most of the data were in Level 3. The tube with corrugations in Ganeshan and Raja [34] has the highest efficiency index. The data were mostly in Region 3 for the tubes with dimples and different types of roughness. There is a clear trend that when the Re increases, the efficiency index decreases. It indicated that these tubes were mostly suitable for lower Reynolds number. The tube in Rabas et al. [48] with dimples has the highest efficiency index.

With the aid of the plot, we can easily observe the efficiency of different types of heat transfer augmentation techniques. For a specific type of augmentation technique, we can also observe which Reynolds number regime is most effective.

3.2. Different types of fins for air

The airside thermal resistance is normally rather important for the fin and tube heat exchangers. Therefore, different types of fins were developed. The typical fins to enhance the heat transfer include wavy, vortex generator, and louver structures [56].

In order to demonstrate how to use the method to evaluate the efficiency of fin and tube heat exchangers, the data in Wang et al. [57] is taken as an example. In the evaluation, the plain fin is considered as the reference surface. The formulas for fitting of experimental data for plain fins are used to determine m_1 and m_2.

$$f_r(Re) = 4.782Re^{-0.654} \tag{34}$$

$$Nu_r(Re) = 0.536Re^{0.474} \tag{35}$$

From the equation, $m_1 = -0.654$ and $m_2 = 0.474$.

$$k_P = \frac{m_2}{3+m_1} = 0.202, \quad k_{\Delta p} = \frac{m_2}{2+m_1} = 0.352, \quad k_V = 1.0$$

The performance evaluation plot for the different types of fins in Wang et al. [57] is shown in Fig. 7. As shown in the figure, the experimental data with lower Reynolds number has higher levels of efficiency. As the *Re* increases, the efficiency decreases. Most of data were in the region of Level 3, when Reynolds number is higher than 1000. For the four types of fins, it is obvious that the convex-louver fins have higher efficiency. The nominal heat transfer area for the four types of fins was the same, the fin pitch was 2.5 mm, outside tube diameters were 10.06 mm, number of rows was 2, and other geometric parameters were all the same. As shown in the figure, convex-louver fin has higher energy efficiency levels based on the comparison (see Fig. 8).

Fig. 2. Photos of heat transfer enhancement techniques for internal pipe flow.

Table 1
Experimental data for internally finned tubes.

Researcher	Re	Fluid	Tube/number	Best tube /Feature	f/f_p	Nu/Nu_p
Webb et al. [16] (1971)	6–100 × 10^3	Air	Low-Fin/5	e/d_i = 0.04, d_i = 38.6 p/e = 10, α = 90°	6.8–14.4	2.4–2.8
Gee and Webb [17] (1980)	6–65 × 10^3	Air	Low-Fin/3	e/d_i = 0.01, d_i = 25.4 p/e = 15, α = 70°	1.5–2.1	1.4–1.6
Han [18] (1984)	7–90 × 10^3	Air	High-Fin/5	e/d_i = 0.21, d_h = 70 p/e = 6, α = 90°	4.3–6.5	1.9–2.5
Wang et al. [10] (1996)	2.5–40 × 10^3	Water	Micro-fin/7	e/d_i = 0.022, Ns = 60 p/e = 7.22, α = 18°	1.5–2.2	0.8–2.1
Brognaux et al. [11] (1997)	2.5–50 × 10^3	Water	Micro-fin/6	e/d_i = 0.036, Ns = 78 p/e = 1.66, α = 20°	1.1–1.7	1.6–1.8
Jensen & Vlakancic [19] (1999)	13–70 × 10^3	Water, EG	Micro-fin/8 Highfin/7	e/d_i = 0.014, Ns = 54 α = 45°	2.1–2.4	3.0–3.7
Tao et al. [20] (2000)	5–50 × 10^3	Air	High-Fin/5	e/d_i = 0.375, Ns = 9 p/e = 2.81, α = 0°	3.6–3.8	2.7–3.5
Webb et al. [12] (2000)	20–60 × 10^3	Water	Micro-fin/7	e/d_i = 0.021, Ns = 45 p/e = 2.81, α = 45°	2.1–2.4	2.2–2.3
Layek et al. [21] (2007)	3–21 × 10^3	Air	Micro-fin/6	e/d_i = 0.03, p/e = 6	2.7–3.5	2.3–2.9
Ji et al. [1] (2012)	10–100 × 10^3	Water	Micro-fin/16	e/d_i = 0.021, Ns = 45 α = 40°	2.9–3.2	2.9

Table 2
Experimental data for inserted twisted tape and coils.

Researcher	Re	Fluid	Tube/number	Best Tube/Feature	f/f_p	Nu/Nu_p
Smithberg and Landis [22] (1964)	5–50 × 10^3	Air, water	Twisted tape/5	y = 3.62	2.2–2.7	2.3–2.7
Lopina and Bergles [23] (1969)	8–130 × 10^3	Water	Twisted tape/5	y = 2.48	1.1–1.7	3.4–4.3
Bergles et al. [24] (1969)	13–70 × 10^3	Water	Twisted tapes in roughed tube/3	y = 2.55	4.9–7.0	1.6–2.0
Saha et al. [25] (1990)	5–43 × 10^3	Water	Twisted tape/16	y = 10, space ratio = 2.5	2.9–3.6	1.2–3.6
Yilmaz et al. [26] (1999)	20–120 × 10^3	Air	Vane swirl generator/5	Vane angle 75°	18.7–20.1	1.8–2.2
Liao and Xin [27] (2000)	16–48 × 10^3	Water, EG, oil	Twisted-tape in roughed tubes/12	p/d_i = 5	6.4–7.1	1.6–2.2
Wang and Sunden [28] (2002)	100–600 5–45 × 10^3	Air	Twisted-tape and coil /9	y = 0.42	45.4–46.7 22.8–23.6	2.0–6.7 3.3–3.4
Chang et al. [29] (2007)	5–25 × 10^3	Air Water	Twisted-tape and coil/9 Serrated twisted tape/8	y = 0.42 y = 1.56	48.7–79.8	3.7–4.8
Promvonge [30] (2007)	6–26 × 10^3	Air	Conical-ring and twisted tape insert/3	y = 3.75	165–170	3.7–6.5
Bas and Ozceyhan [31] (2012)	5.1–25 × 10^3	Air	Twisted tapes/10	y = 2.0	3.1–4.1	1.9–2.6
Bhuiya et al. [32] (2016)	7–50 × 10^3	Air	Perforated double counter twisted tapes/4	Porosity = 4.6%, y = 1.92	2.4–4.0	2.3–3.5

Table 3
Experimental data for corrugated or twisted tubes.

Researcher	Re	Fluid	Tube/number	Best tube/Feature	f/f_p	Nu/Nu_p
Kidd [33] (1970)	20–260 × 10^3	Air	Corrugated/9	p/d_i = 0.8, e/d_i = 0.037	1.6–1.7	1.3–1.5
Ganeshan&Raja Rao [34] (1982)	50–90 × 10^3	Water, polymer solutions	Corrugated/7	p/d_i = 1.169, e/d_i = 0.0261	1.9–2.4	1.8–2.6
Sethumadhavan and Raja Rao [35] (1986)	10–80 × 10^3	Water, EG	Multi starts corrugated /5	p/d_i = 0.297, e/d_i = 0.023, N_s = 4	2.6–3.3	1.6–1.8
Obot et al. [36] (1992)	0.7–50 × 10^3	Air	Corrugated/3	p/d_i = 0.2, e/d_i = 0.056	1.8–3.0	1.8–2.2
Esen et al. [37] (1994)	0.6–44 × 10^3	Air	Corrugated/23	p/d_i = 0.522, e/d_i = 0.066	2.7–3.6	1.7–2.3
Chen et al. [38] (2001)	10–25 × 10^3	Water	Four starts spiral/9	p/d_i = 0.48, e/d_i = 0.12	3.7–4.5	2.5–3.8
Cui et al. [39] (2003)	8–30 × 10^3	Water	Corrugated/6	p/d_i = 0.3129, e/d_i = 0.0409	3.3–3.9	1.9–2.8
Li et al. [40] (2006)	8–50 × 10^3	Air	Alternating elliptical tube/1	p/d_i = 2.94	1.75–1.9	1.6–1.9
Bilen et al. [41] (2009)	10–38 × 10^3	Air	Wavy/3	p/d_i = 0.333, e/d_i = 0.083	1.5–2.8	1.4–1.7
Fernandez-Seara&Uhia [42] (2012)	10–100 × 10^3	Water	Corrugated/9	p/d_i = 0.556, e/d_i = 0.044	4.3–4.9	2.1–2.4
García et al. [43] (2012)	0.1–100 × 10^3	Water	Corrugated/3	p/d_i = 0.886, e/d_i = 0.057	1.8–3.8	1.4–2.3
Poredos et al. [44] (2013)	2–12 × 10^3	Air	Corrugated/7	Corrugation ratio = 1.401	7.2–9.4	1.7–1.9
Nelly et al. [45] (2015)	4–20 × 10^3	Air	Corrugated tube/7	p/d_i = 0.34, e/d_i = 0.043	4.0–5.4	1.6–1.8
Harleß et al. [46] (2016)	5–23 × 10^3	Air	Corrugated tube/18	p/d_i = 0.8, e/d_i = 0. 046	2.8–3.7	1.8–2.1

Table 4
Experimental data for dimpled and three dimensional roughed tubes.

Researcher	Re	Fluid	Tube/number	Best tube/Feature	f/f_p	Nu/Nu_p
Gowen&Smith [47] (1968)	$6–100 \times 10^3$	Air, water, ethylene glycol	Sand roughness /8	$e/d_i = 0.026$	3.5–5.8	2.3–3.3
Rabas et al. [48] (1993)	$10–60 \times 10^3$	Water	Dimpled/2	$p/d_i = 1.448$, $e/d_i = 0.0173$	1.5–1.9	1.5–1.6
Liao and Xin [49] (1995)	$0.25–7 \times 10^3$	Ethylene glycol	Extended protrusions/7	$p_d/d_i = 0.32$, $p_c/d_i = 0.179$, $e/d_i = 0.04$	1.7–4.4	2.6–4.5
Olsson and Sunden [50] (1996)	$0.5–6 \times 10^3$	Air	Dimpled/5	$p/d_i = 1.708$, $e/d_i = 0.16$	3.6–4.5	2.5–4.2
Liao et al. [27] (2000)	$5–80 \times 10^3$	Water, ethylene glycol	Extended protrusions /14	$p_d/di = 3.98$, $e/d_i = 0.098$	3.8–4.4	2.9–3.6
Chen et al. [51] (2001)	$7.5–52 \times 10^3$	Water	Dimpled/6	$p/d_i = 0.602$, $e/d_i = 0.078$ $N_s = 6$	3.3–4.8	2.1–2.8
Vicente et al. [52] (2002)	$10–100 \times 10^3$	Water, ethylene glycol	Dimpled/10	$p/d_i = 0.819$, $e/d_i = 0.0988$	3.1–3.5	1.3–2.0
Vicente et al. [53] (2002)	$2–100 \times 10^3$	Water, ethylene glycol	Dimpled/10	$p/d_i = 0.906$, $e/d_i = 0.114$	3.2–4.2	1.5–2.5
Bunker and Donnellan [54] (2003)	$20–50 \times 10^3$	Air	Dimpled/6	$e/d_i = 0.107$	5.6–7.4	1.9–2.1
Li et al. [55] (2009)	$15–60 \times 10^3$	Water	Discrete ribs/1	$p/d_i = 0.32$, $e/d_i = 0.02$	2.8–3.5	2.0–2.1
Webb [41] (2009)	$4–24 \times 10^3$	Water	Coned/3	$p_d/d_i = 3.95$, $p_c/di = 7.21$, $e/d_i = 0.025$	3.6–4.6	2.6–4.5

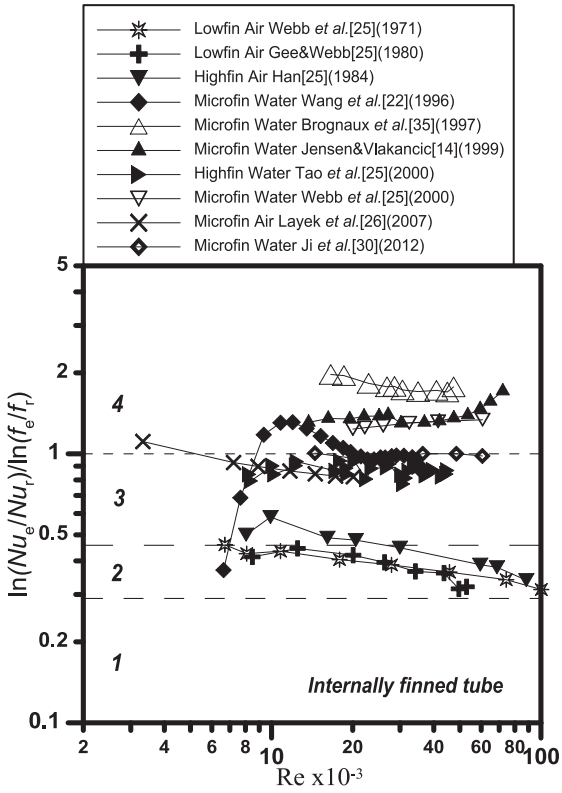

Fig. 3. Performance evaluation plot for internally finned tubes.

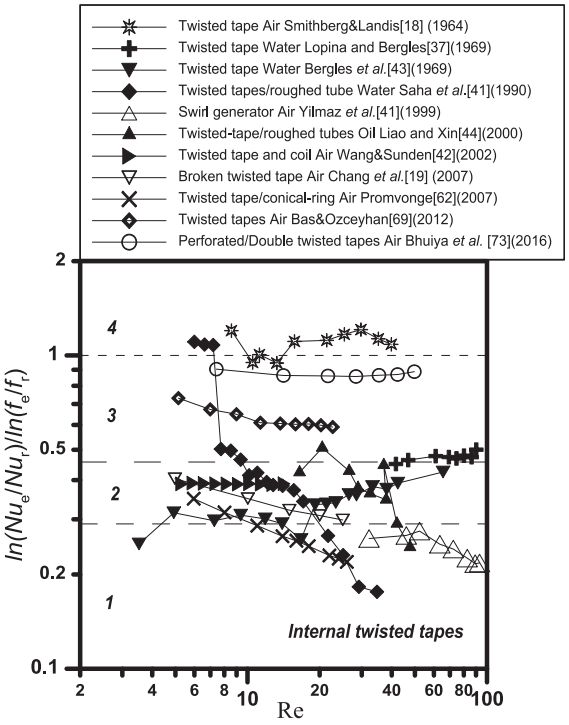

Fig. 4. Performance evaluation plot for internal twisted tape or coil inserts.

3.3. Shell and tube heat exchanger

Efficiency of shell-and-tube heat exchangers could be improved using different types of baffles [58,59]. A lot of experimental investigations were conducted for the segmental and helical baffles. We can also evaluate this kind of heat exchangers using the performance evaluation method. The heat exchangers in comparison should be based on the same four assumptions. The diameter of tubes, tube pitch and number, and shell diameter should be the same.

To give an example, the experimental data with different types of baffles in Zhang et al. [60] is evaluated. In the evaluation, the helical baffle with the angle of 20° is used as the reference surface. The formulas for fitting of experimental data for the 20° helical baffled heat exchanger are collected to determine m_1 and m_2.

$$f_r(Re) = 13.571 Re^{-0.751} \tag{36}$$

$$Nu_r(Re) = 0.290 Re^{0.534} \tag{37}$$

From the equation, $m_1 = -0.751$ and $m_2 = 0.534$.

$$k_P = \frac{m_2}{3+m_1} = 0.237, \quad k_{\Delta p} = \frac{m_2}{2+m_1} = 0.428, \quad k_V = 1.0$$

As shown in Fig. 9, the segmental baffle in comparison has higher efficiency. It has the same heat transfer areas for the two heat exchangers and the layout of tubes are the same. Although

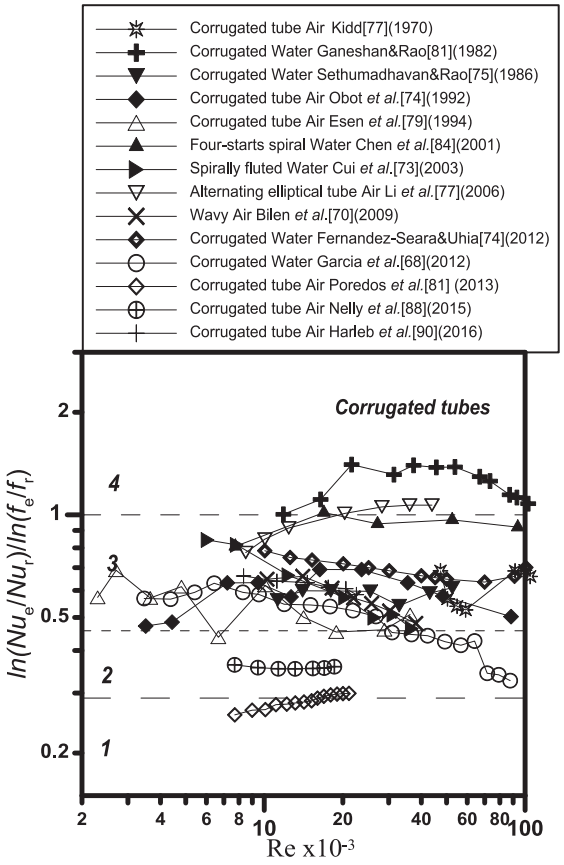

Fig. 5. Performance evaluation plot for corrugated tubes.

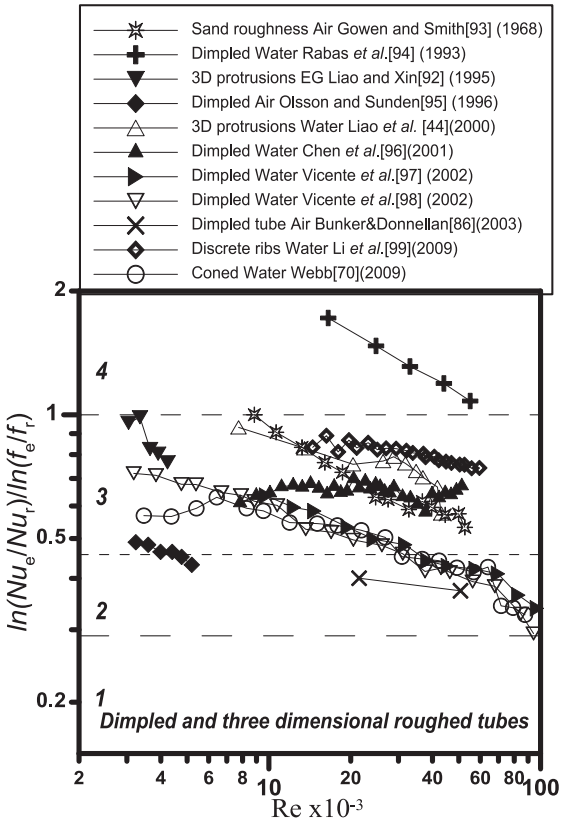

Fig. 6. Performance evaluation plot for dimpled and three dimensional roughed tubes.

the heat transfer performance for segmental baffled heat exchanger is higher at the same Reynolds number, it has higher energy saving efficiency at the constraints of same pressure drop.

To further augment the heat transfer of such kind of heat exchangers, the enhanced tubes such as finned, corrugated, and other enhancement techniques were also used [61–65]. The tube-side enhancement techniques can also be evaluated with the proposed performance evaluation method.

3.4. Plate heat exchangers

For heating and cooling applications, plate heat exchanger was also extensively used. Different types of plates were manufactured to intensify the heat transfer of single or two phase flow. Corrugation inclination angle is an important parameter for the plate. The changes in inclination angles affect the friction factor and heat transfer.

To give an example, the experimental data of the plate with different inclination angle in Focke et al. [66] was also evaluated with the performance evaluation method. The merit can also be evaluated for the energy saving purposes.

In the evaluation, the corrugation inclination angle of 30° is regarded as the reference surface. The formulas for fitting of experimental data of the reference surface are:

$$f_r(Re) = 4.405Re^{-0.289} \tag{38}$$

$$Nu_r(Re) = c_2 Re^{0.649} \tag{39}$$

From the equation, $m_1 = -0.289$ and $m_2 = 0.649$,

$$k_P = \frac{m_2}{3+m_1} = 0.239, \quad k_{\Delta p} = \frac{m_2}{2+m_1} = 0.379, \quad k_V = 1.0$$

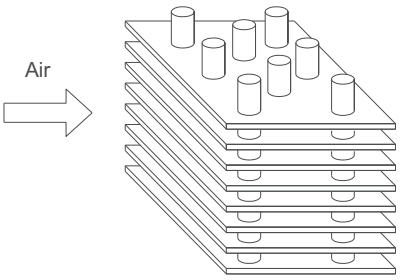

Fig. 7. Schematic of fin and tube heat exchangers.

As shown in Fig. 10, the reference surface is that with inclination angle of 30°. At lower and higher Reynolds number, the plates with inclination angle of 45° had lower efficiency compared with that of 30°. While at the Reynolds number of 300 to 3000, the efficiency index was higher compared with other angles. At the Reynolds number of 300 to 3000, most of data were in Level 2. The decrease of efficiency at higher Reynolds was because the increment ratio of heat transfer was lower than the increment rate of friction factor.

This article only provides some typical examples for using the evaluation method. It is required that the four assumptions should be satisfied for different cases. Normally, one compares the performance of an enhanced surface with that of the corresponding reference (e.g. plain or smooth) surfaces. The evaluation method in this work can aid this comparison. Compared with the assessment method presented by Fan et al. [8], the evaluation method in this paper may complement each other. Take the plate heat exchanger as an example, the performance plot of Fan et al. [8] is show in Fig. 11. As the increase of corrugation inclination angle, the friction

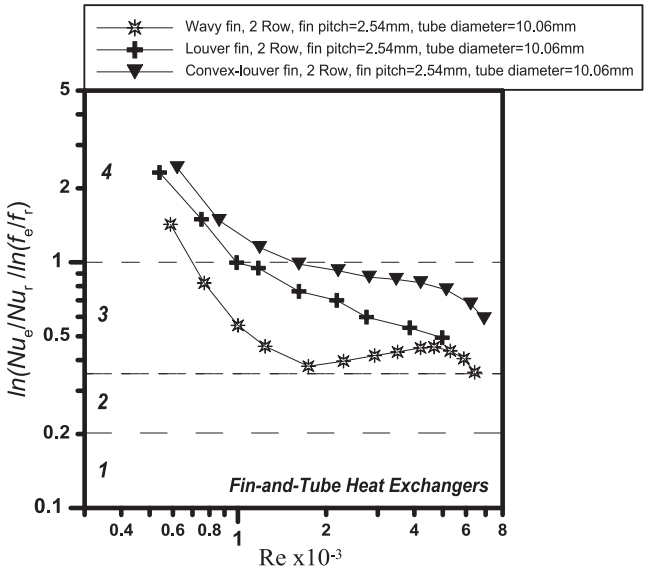

Fig. 8. Performance evaluation plot for fin and tube heat changers with different types of fins.

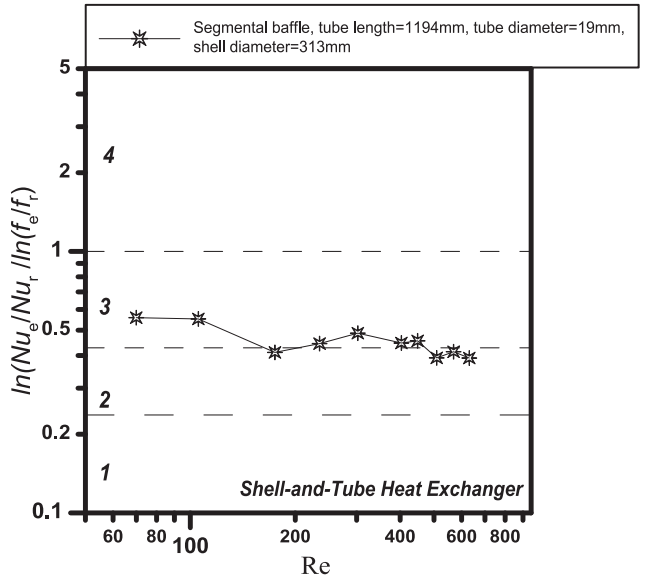

Fig. 9. Performance evaluation plot for shell and tube heat exchangers with different types of baffles.

factor also increases. Experimental data were mostly in Region 1 and Region 2. Although we can tell which Region it is located in, it is hard to observe the variation of heat transfer performance with the changes of Reynolds number. The levels of efficiency are also a little bit difficult to observe from the plot. Moreover, the plot for Fan et al. [8] is based on the assumptions of same temperature difference for the reference and enhanced surface. This assumption was removed for the present method. As the thermophysical properties, heat transfer area, nominal flow area, characteristic length for the reference and enhanced surfaces, and temperature of fluid at the inlet are the same, if the Nusselt number is increased, the heat transfer would also be intensified. By simply compare the Nusselt number at the different constraints, the energy saving efficiency of different surface can be identified.

It should be noted that different forms of the efficiency indexes (η) have been proposed in the literature. The most widely used

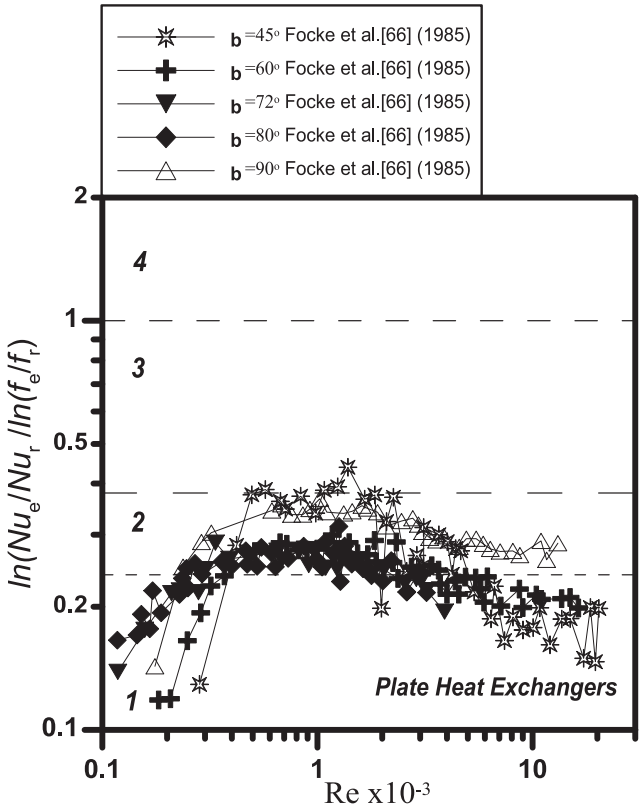

Fig. 10. Performance evaluation plot for plate heat exchangers with different corrugation inclination angles.

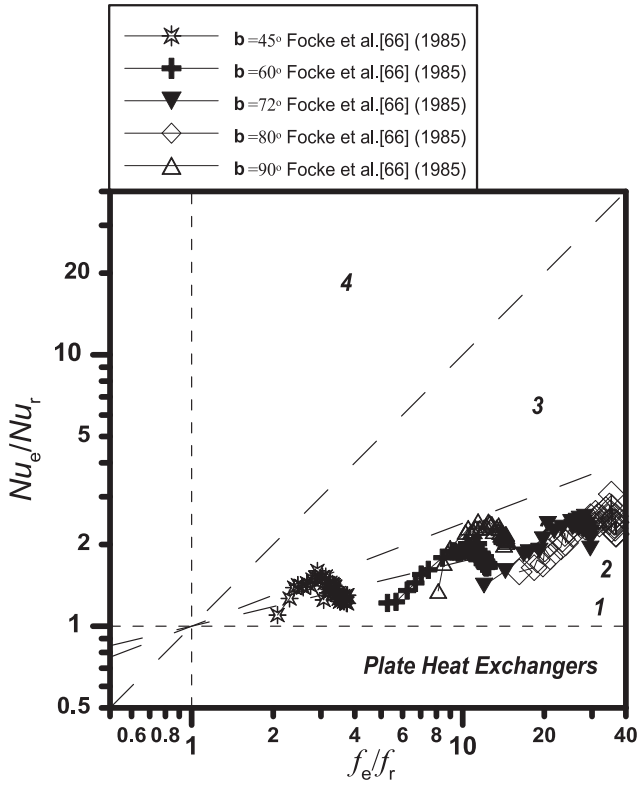

Fig. 11. Performance plot proposed by Fan et al. [8] for plate heat exchanger.

criterion $k_i = 1/3$ was developed by Webb and Eckert [7], $\eta = \frac{Nu_e}{Nu_r} / \left(\frac{f_e}{f_r}\right)^{1/3}$. Simply comparing the increase of Nusselt number over friction factor relative to the referenced surface at identical flow rate, $k_i = 1$ for $\eta = \frac{Nu_e}{Nu_r} / \frac{f_e}{f_r}$, was also widely used [10]. $k_i = 1/2$ for $\eta = \frac{Nu_e}{Nu_r} / \left(\frac{f_e}{f_r}\right)^{1/2}$ and $k_i = 1/6$ for $\eta = \frac{Nu_e}{Nu_r} / \left(\frac{f_e}{f_r}\right)^{1/6}$ were also found to be used in [67] and [68], respectively. Which index is better, 1, 1/2, or 1/3? [69]. While the efficiency index $k_i = \ln\left(\frac{Nu_e}{Nu_r}\right) / \ln\left(\frac{f_e}{f_r}\right)$, presented in this work, as a unified criteria can be used to identify the effectiveness of different heat transfer augmentation techniques in one evaluation plot. The plot is separated into different regions with k_i, and the levels of efficiency can also be easily identified.

4. Conclusions

In order to assess the energy saving effectiveness of an enhanced surface, an evaluation method was proposed in this paper. The efficiency for the augmented surface can be easily identified via a plot. In the plot, Reynolds number and the efficiency index $k_i = \ln\left(\frac{Nu_e}{Nu_r}\right) / \ln\left(\frac{f_e}{f_r}\right)$ were taken as the X and Y coordinates, respectively. Compared with four assumptions made in [8], it is more reasonable for practical situation. The effect of Reynolds number was also explicitly reflected.

The performance evaluation plot can be divided into four typical levels. The data falls into the region of Level 1 is featured by intensified heat transfer and more energy consumption. Data in Level 2 is that the heat transfer could be intensified at the same pump power. In Level 3, it is characterized by the enhanced heat transfer at the same pressure drop. The efficiency in Level 4 is the highest. In this region, the increase of heat transfer is more than the increase of friction factor at the same flow rate. Experimental data that located in higher levels in the coordinate will be more effective in energy saving. Through the examples, it showed that this method can be employed to evaluate the efficiency of different heat transfer augmentation techniques or heat exchangers for energy saving purpose.

Conflict of interest

Author declares that there is no conflict of interest.

Acknowledgment

This work was supported by the National Natural Science Foundation of China (51776160) and National Key R&D Program of China (No. 2016YFB0601200).

References

[1] B.S. Petukhov, Heat transfer and friction in turbulent pipe flow with variable physical properties, Adv. Heat Transf. 6 (1970) 503–564.
[2] V. Gnielinski, New equations for heat and mass transfer in turbulent pipe and channel flows, Int. J. Chem. Eng. 16 (1976) 359–368.
[3] W.T. Ji, D.C. Zhang, Y.L. He, W.Q. Tao, Prediction of fully developed turbulent heat transfer of internal helically ribbed tubes-An extension of Gnielinski equation, Int. J. Heat Mass Transf. 55 (4) (2011) 1375–1384.
[4] V. Zimparov, Extended performance evaluation criteria for enhanced heat transfer surfaces: heat transfer through ducts with constant wall temperature, Int. J. Heat Mass Transf. 43 (17) (2000) 3137–3155.
[5] R.L. Webb, Performance evaluation criteria for use of enhanced heat transfer surfaces in heat exchanger design, Int. J. Heat Mass Transf. 24 (4) (1981) 715–726.
[6] B. Yu, J. Nie, Q. Wang, W. Tao, Experimental study on the pressure drop and heat transfer characteristics of tubes with internal wave-like longitudinal fins, Heat Mass Transf. 35 (1) (1999) 65–73.
[7] R.L. Webb, E.R.G. Eckert, Application of rough surfaces to heat exchanger design, Int. J. Heat Mass Transf. 15 (9) (1972) 1647–1658.
[8] J.F. Fan, W.K. Ding, J.F. Zhang, Y.L. He, W.Q. Tao, A performance evaluation plot of enhanced heat transfer techniques oriented for energy-saving, Int. J. Heat Mass Transf. 52 (1) (2009) 33–44.
[9] A. Bejan, A.D. Kraus, Heat transfer handbook, John Wiley & Sons, 2003.
[10] C.C. Wang, C. Chiou, D.C. Lu, Single-phase heat transfer and flow friction correlations for microfin tubes, Int. J. Heat Fluid Flow 17 (5) (1996) 500–508.
[11] L.J. Brognaux, R.L. Webb, L.M. Chamra, B.Y. Chung, Single-phase heat transfer in micro-fin tubes, Int. J. Heat Mass Transf. 40 (18) (1997) 4345–4357.
[12] R.L. Webb, R. Narayanamurthy, P. Thors, Heat transfer and friction characteristics of internal helical-rib roughness, ASME J. Heat Transf. 122 (1) (2000) 134–142.
[13] W.T. Ji, D.C. Zhang, N. Feng, J.F. Guo, M. Numata, G.N. Xi, W.Q. Tao, Nucleate pool boiling heat transfer of R134a and R134a-PVE lubricant mixtures on smooth and five enhanced tubes, J. Heat Transf. 132 (11) (2010) 11502.
[14] W.-T. Ji, A.M. Jacobi, Y.-L. He, W.-Q. Tao, Summary and evaluation on single-phase heat transfer enhancement techniques of liquid laminar and turbulent pipe flow, Int. J. Heat Mass Transf. 88 (2015) 735–754.
[15] W.-T. Ji, A.M. Jacobi, Y.-L. He, W.-Q. Tao, Summary and evaluation on the heat transfer enhancement techniques of gas laminar and turbulent pipe flow, Int. J. Heat Mass Transf. 111 (2017) 467–483.
[16] R.L. Webb, E.R.G. Eckert, R.J. Goldstein, Heat transfer and friction in tubes with repeated-rib roughness, Int. J. Heat Mass Transf. 14 (4) (1971) 601–617.
[17] D.L. Gee, R. Webb, Forced convection heat transfer in helically rib-roughened tubes, Int. J. Heat Mass Transf. 23 (8) (1980) 1127–1136.
[18] J. Han, Heat transfer and friction in channels with two opposite rib-roughened walls, J. Heat Transf. 106 (4) (1984) 774–781.
[19] M.K. Jensen, A. Vlakancic, Experimental investigation of turbulent heat transfer and fluid flow in internally finned tubes, Int. J. Heat Mass Transf. 42 (7) (1999) 1343–1351.
[20] W.-Q. Tao, S.-S. Lu, H. Kang, M. Lin, Experimental study on developing and fully developed fluid flow and heat transfer in annular-sector ducts, J. Enhanced Heat Transf. 7 (1) (2000).
[21] A. Layek, J. Saini, S. Solanki, Heat transfer and friction characteristics for artificially roughened ducts with compound turbulators, Int. J. Heat Mass Transf. 50 (23) (2007) 4845–4854.
[22] E. Smithberg, F. Landis, Friction and forced convection heat-transfer characteristics in tubes with twisted tape swirl generators, ASME J. Heat Transf. 86 (1) (1964) 39–48.
[23] R. Lopina, A. Bergles, Heat transfer and pressure drop in tape-generated swirl flow of single-phase water, J. Heat Transf. 91 (3) (1969) 434–441.
[24] A. Bergles, R. Lee, B. Mikic, Heat transfer in rough tubes with tape-generated swirl flow, ASME J. Heat Transf. 91 (3) (1969) 443–445.
[25] S. Saha, U. Gaitonde, A. Date, Heat transfer and pressure drop characteristics of turbulent flow in a circular tube fitted with regularly spaced twisted-tape elements, Exp. Therm. Fluid Sci. 3 (6) (1990) 632–640.
[26] M. Yilmaz, Ö. Çomakli, S. Yapici, Enhancement of heat transfer by turbulent decaying swirl flow, Energy Convers. Manage. 40 (13) (1999) 1365–1376.
[27] Q. Liao, M. Xin, Augmentation of convective heat transfer inside tubes with three-dimensional internal extended surfaces and twisted-tape inserts, Chem. Eng. J. 78 (2) (2000) 95–105.
[28] L. Wang, B. Sunden, Performance comparison of some tube inserts, Int. Commun. Heat Mass Transf. 29 (1) (2002) 45–56.
[29] S.W. Chang, Y.J. Jan, J.S. Liou, Turbulent heat transfer and pressure drop in tube fitted with serrated twisted tape, Int. J. Therm. Sci. 46 (5) (2007) 506–518.
[30] P. Promvonge, S. Eiamsa-ard, Heat transfer behaviors in a tube with combined conical-ring and twisted-tape insert, Int. Commun. Heat Mass Transf. 34 (7) (2007) 849–859.
[31] H. Bas, V. Ozceyhan, Heat transfer enhancement in a tube with twisted tape inserts placed separately from the tube wall, Exp. Therm. Fluid Sci. 41 (2012) 51–58.
[32] M.M.K. Bhuiya, A.K. Azad, M.S.U. Chowdhury, M. Saha, Heat transfer augmentation in a circular tube with perforated double counter twisted tape inserts, Int. Commun. Heat Mass Transf. 74 (2016) 18–26.
[33] G. Kidd, The heat transfer and pressure-drop characteristics of gas flow inside spirally corrugated tubes, J. Heat Transf. 92 (3) (1970) 513–518.
[34] S. Ganeshan, M.R. Rao, Studies on thermohydraulics of single-and multi-start spirally corrugated tubes for water and time-independent power law fluids, Int. J. Heat Mass Transf. 25 (7) (1982) 1013–1022.
[35] R. Sethumadhavan, M.R. Rao, Turbulent flow friction and heat transfer characteristics of single-and multistart spirally enhanced tubes, ASME J. Heat Transf. 108 (1) (1986) 55–61.
[36] N. Obot, E. Esen, K. Snell, T. Rabas, Pressure drop and heat transfer characteristics for air flow through spirally fluted tubes, Int. Commun. Heat Mass Transf. 19 (1) (1992) 41–50.
[37] E. Esen, N. Obot, T.J. Rabas, Enhancement: Part I. Heat transfer and pressure drop results for air flow through passages with spirally-shaped roughness, J. Enhanced Heat Transf. 1 (2) (1994).
[38] X. Chen, X. Xu, S. Nguang, A.E. Bergles, Characterization of the effect of corrugation angles on hydrodynamic and heat transfer performance of four-start spiral tubes, ASME J. Heat Transf. 123 (6) (2001) 1149–1158.
[39] H. Cui, X. Yuan, Z. Yao, Experimental investigation of heat transfer and pressure drop characteristics of w-type spirally fluted tubes, Exp. Heat Transf. 16 (3) (2003) 159–169.

[40] B. Li, B. Feng, Y.-L. He, W.-Q. Tao, Experimental study on friction factor and numerical simulation on flow and heat transfer in an alternating elliptical axis tube, Appl. Therm. Eng. 26 (17) (2006) 2336–2344.
[41] K. Bilen, M. Cetin, H. Gul, T. Balta, The investigation of groove geometry effect on heat transfer for internally grooved tubes, Appl. Therm. Eng. 29 (4) (2009) 753–761.
[42] J. Fernández-Seara, F.J. Uhía, Heat transfer and friction characteristics of spirally corrugated tubes for outer ammonia condensation, Int. J. Refrig. 35 (7) (2012) 2022–2032.
[43] A. Garcia, J. Solano, P. Vicente, A. Viedma, The influence of artificial roughness shape on heat transfer enhancement: corrugated tubes, dimpled tubes and wire coils, Appl. Therm. Eng. 35 (2012) 196–201.
[44] P. Poredoš, T. Šuklje, S. Medved, C. Arkar, An experimental heat-transfer study for a heat-recovery unit made of corrugated tubes, Appl. Therm. Eng. 53 (1) (2013) 49–56.
[45] S.M. Nelly, W. Nieratschker, M. Nadler, D. Raab, A. Delgado, Experimental and numerical investigation of the pressure drop and heat transfer coefficient in corrugated tubes, Chem. Eng. Technol. 38 (12) (2015) 2279–2290.
[46] A. Harleß, E. Franz, M. Breuer, Experimental investigation of heat transfer and friction characteristic of fully developed gas flow in single-start and three-start corrugated tubes, Int. J. Heat Mass Transf. 103 (2016) 538–547.
[47] R. Gowen, J. Smith, Turbulent heat transfer from smooth and rough surfaces, Int. J. Heat Mass Transf. 11 (11) (1968) 1657–1674.
[48] T.J. Rabas, R.L. Webb, P. Thors, N.-K. Kim, Influence of roughness shape and spacing on the performance of three-dimensional helically dimpled tubes, J. Enhanced Heat Transf. 1 (1) (1993).
[49] Q. Liao, M. Xin, Experimental investigation on forced convective heat transfer and pressure drop of ethylene glycol in tubes with three-dimensional internally extended surface, Exp. Therm. Fluid Sci. 11 (4) (1995) 343–347.
[50] C.-O. Olsson, B. Sunden, Heat transfer and pressure drop characteristics of ten radiator tubes, Int. J. Heat Mass Transf. 39 (15) (1996) 3211–3220.
[51] J. Chen, H. Müller-Steinhagen, G.G. Duffy, Heat transfer enhancement in dimpled tubes, Appl. Therm. Eng. 21 (5) (2001) 535–547.
[52] P.G. Vicente, A. García, A. Viedma, Experimental study of mixed convection and pressure drop in helically dimpled tubes for laminar and transition flow, Int. J. Heat Mass Transf. 45 (26) (2002) 5091–5105.
[53] P.G. Vicente, A. Garćıa, A. Viedma, Heat transfer and pressure drop for low Reynolds turbulent flow in helically dimpled tubes, Int. J. Heat Mass Transf. 45 (3) (2002) 543–553.
[54] R.S. Bunker, K.F. Donnellan, Heat transfer and friction factors for flows inside circular tubes with concavity surfaces, in: ASME Turbo Expo 2003, collocated with the 2003 International Joint Power Generation Conference, American Society of Mechanical Engineers, 2003, pp. 21–29.
[55] X.-W. Li, J.-A. Meng, Z.-Y. Guo, Turbulent flow and heat transfer in discrete double inclined ribs tube, Int. J. Heat Mass Transf. 52 (3) (2009) 962–970.
[56] C.-C. Wang, On the airside performance of fin-and-tube heat exchangers, in: Heat Transfer Enhancement of Heat Exchangers, Springer, 1999, pp. 141–162.
[57] C. Wang, P. Chen, J. Jang, Heat transfer and friction characteristics of convex-louver fin-and-tube heat exchangers, Exp. Heat Transf. 9 (1) (1996) 61–78.
[58] W.-T. Ji, C.-Y. Zhao, J. Lofton, Z. Li, D.-C. Zhang, Y.L. He, W.-Q. Tao, Condensation of R134a and R22 in shell and tube condensers mounted with high-density low-fin tubes, J. Heat Transf. (2018).
[59] J. Lutcha, J. Nemcansky, Performance improvement of tubular heat exchangers by helical baffles, Chem. Eng. Res. Des. 68 (3) (1990) 263–270.
[60] J.-F. Zhang, B. Li, W.-J. Prin, Y.-G. Lei, Y.-L. He, W.-Q. Tao, Experimental performance comparison of shell-side heat transfer for shell-and-tube heat exchangers with middle-overlapped helical baffles and segmental baffles, Chem. Eng. Sci. 64 (8) (2009) 1643–1653.
[61] Z. Zhang, X. Fang, Comparison of heat transfer and pressure drop for the helically baffled heat exchanger combined with three-dimensional and two-dimensional finned tubes, Heat Transf. Eng. 27 (7) (2006) 17–22.
[62] S. Rozzi, R. Massini, G. Paciello, G. Pagliarini, S. Rainieri, A. Trifiro, Heat treatment of fluid foods in a shell and tube heat exchanger: comparison between smooth and helically corrugated wall tubes, J. Food Eng. 79 (1) (2007) 249–254.
[63] W.-T. Ji, C.-Y. Zhao, D.-C. Zhang, Z.-Y. Li, Y.-L. He, W.-Q. Tao, Condensation of R134a outside single horizontal titanium, cupronickel (B10 and B30), stainless steel and copper tubes, Int. J. Heat Mass Transf. 77 (2014) 194–201.
[64] W.-T. Ji, C.-Y. Zhao, Y.-L. He, G.-N. Xi, W.-Q. Tao, Vapor flow effect on falling film evaporation of R134a outside horizontal tube bundle, The 15th International Heat Transfer Conference, Kyoto, Japan, 2014.
[65] C.-Y. Zhao, P.-H. Jin, W.-T. Ji, Y.-L. He, W.-Q. Tao, Experimental investigations of R134a and R123 falling film evaporation on enhanced horizontal tubes, Int. J. Refrig. 75 (2017) 190–203.
[66] W. Focke, J. Zachariades, I. Olivier, The effect of the corrugation inclination angle on the thermohydraulic performance of plate heat exchangers, Int. J. Heat Mass Transf. 28 (8) (1985) 1469–1479.
[67] Y.L. Zhang, J.P. Liu, D.T. Chong, J.J. Yan, Experimental investigation on the heat transfer and flow performances of the fin array with shield in bypass, Int. J. Heat Mass Transf. 56 (1) (2013) 674–682.
[68] F. Xing, J. Xie, J. Xu, Modulated heat transfer tube with mesh cylinder inserted, Int. Commun. Heat Mass Transf. 56 (2014) 15–24.
[69] J. Liu, G. Xie, T.W. Simon, Turbulent flow and heat transfer enhancement in rectangular channels with novel cylindrical grooves, Int. J. Heat Mass Transf. 81 (2015) 563–577.